Yuzuncu Yil University
Journal of the Institute of Natural & Applied Sciences

Research Article

Investigation of Structural, Elastic, and Piezoelectric Properties of NbSbO$_4$ Crystal

Mehmet ERZEN

Van Yuzuncu Yil University, Institute of Natural and Applied Sciences, Department of Physics, 65080, Van, Türkiye

Mehmet ERZEN, ORCID No: 0000-0002-7716-8608
Corresponding author e-mail: merzennn@gmail.com

Abstract: The structural, elastic, and piezoelectric properties of the NbSbO$_4$ crystal were calculated based on the density functional theory. These properties were calculated using the ABINIT package program under both the generalized gradient approximation and the local density approximation. The elastic stiffness tensor and the elastic compliance tensor for the NbSbO$_4$ crystal were calculated in the ground state. Voigt Bulk Modulus, Reuss Bulk Modulus, Hill Bulk Modulus, Voigt Shear Modulus, Reuss Shear Modulus, Hill Shear Modulus, Young Modulus, Poisson Ratio, Flexibility Coefficient, Debye temperature, Longitudinal sound wave velocity for NbSbO$_4$ crystal using elastic stiffness and elastic compliance tensor, Transverse sound wave velocity and Average speed of sound were calculated. Then, the ground state piezoelectric tensor of the NbSbO$_4$ crystal was calculated. Accordingly, 2D longitudinal surfaces and 3D representation surfaces of the piezoelectric tensor were obtained using MTEX software. The properties obtained with both the generalized gradient approximation and the local density approximation are compared. As a result of the calculations, it was understood that the material was a flexible and formable material in both approximations.

NbSbO$_4$ Kristalinin Yapısal, Elastik ve Piezoelektrik Özelliklerinin İncelenmesi

Öz: NbSbO$_4$ kristalinin yapısal, elastik ve piezoelektrik özellikleri, yoğunluk fonksiyonel teorisine dayalı olarak hesaplandı. Bu özellikler için hesaplamalar hem genelleştirilmiş gradyent hem de yerel yoğunluk yaklaşımı altında ABINIT paket programı kullanılarak yapılmıştır. NbSbO$_4$ kristali için elastik sertlik tensörü ve elastik uyum tensörü, temel durumda hesaplanmıştır. Elastik sertlik ve elastik uyum tensörü kullanılarak NbSbO$_4$ kristali için Voigt Bulk Modülü, Reuss Bulk Modülü, Hill Bulk Modülü, Voigt Shear Modülü, Reuss Shear Modülü, Hill Shear Modülü, Young Modülü, Poisson Oranı, Esneklik Katsayısı, Debye sıcaklığı, boyuna ses dalgası hızı, enine ses dalgası hızı ve ortalama ses hızı hesaplanmıştır. Daha sonra NbSbO$_4$ kristalinin temel durumda piezoelektrik tensörü hesaplandı. Buna bağlı olarak, MTEX yazılımı kullanılarak piezoelektrik tensörünün 2 boyutta boyuna yüzeyleri ve 3 boyutta temsil yüzeyleri elde edilmiştir. Hem genelleştirilmiş gradyent yaklaşımı hem de yerel yoğunluk yaklaşımları ile elde edilen özellikler karşılaştırılmıştır. Yapılan hesaplamalar sonucunda malzemenin her iki yaklaşım için de esnek ve şekillendirilebilir bir malzeme olduğu anlaşılmıştır.

1. Introduction

In 1973 Muller and Roy summarized the phase transformations in ABO$_4$ type compounds. They have presented a diagram based on the coordination numbers of both cations versus relative volume change. From the diagram one can see that ABO$_4$ type compounds crystallize in many different structure types, and many different types of phase changes occur in them (Müller & Roy, 1973; Fukunaga & Yamaoka, 1979). The word Piezoelectric comes from Greek, meaning electricity caused by pressure. In the middle of the eighteenth century, Carolus Linnaeus and Franz Aepinus first observed that certain materials, such as crystals and some ceramics, generate electric charges in case of a temperature change. Both René Just Haüy and Antoine César Becquerel subsequently attempted to investigate the phenomena further but were unsuccessful (Dineva et al., 2014). Piezoelectricity as a research field in crystal physics was initiated by the brothers Jacques Curie (1856–1941) and Pierre Curie (1859–1906) with their studies (Curie & Curie, 1880; Dineva et al., 2014). They found that tension and compression produce voltages of opposite polarity and are proportional to the applied load. This phenomenon was called the piezoelectric effect by Hankel (Bouty, 1883). There are many studies on NbSbO$_4$ crystals in the literature. SbNbO$_4$ compound, formed in the ternary system of Nb-Sb-O, was obtained for the first time by high-energy ball milling of an equimolar oxide Sb$_2$O$_3$/Nb$_2$O$_5$ mixture in an argon atmosphere. This compound is X-ray diffraction, differential thermal analysis-thermal gravimetry, characterized by infrared and scanning electron microscopy methods (Dulian et al., 2014). Experimental vibrational spectroscopic study of solid solutions for ferroelectric SbNbO$_4$ and antiferroelectric BiNbO$_4$ crystals was performed (Ayyub et al., 1986). In 1998, thin ferroelectric films of SbNbO$_4$ oriented on Si were synthesized by pulsed laser ablation (Chattopadhyay et al., 1998). The structural properties of the SbNbO$_4$ crystal were obtained using an x-ray/diffractometry (Rannev et al., 1976). The effects of both γ-ray irradiation and annealing temperature on the optical absorption spectra of SbNbO$_4$ films deposited on MgO or quartz substrates in a certain spectral range were investigated (El-Fadl et al., 2003). A study was conducted on the photophysical and photocatalytic water separation performance of SbMO$_4$ (M = Nb, Ta) compounds and some properties such as electronic band structure, and density of state were obtained (Kim et al., 2012). Some thermodynamic properties have been obtained for SbNbO$_4$ and SbSbO$_4$ crystals (Knauth & Schwitzgebel, 1988 and 1990). An experimental study was conducted on the effect of gamma radiation and heat treatment on the optical properties of SbNbO$_4$ ferroelectric thin films. In addition, the structural and optical properties of the SbNbO$_4$ crystal were obtained experimentally (Mohamad et al., 1998 and 2001). The dielectric and nonlinear optical properties of SbNbO$_4$, SbTaO$_4$, BiNbO$_4$ and BiTaO$_4$ crystals were obtained. In addition, structural properties of SbNbO$_4$ and some other crystals were obtained (Popolitov et al., 1974 and 1982). A study was conducted on the first synthesis of oriented SbNbO$_4$ ferroelectric thin films on Pt-coated silicon substrates (Qu & Lévy, 1995). In 2018, a study was conducted on the Electrochemical Reaction of Lithium with the SbNbO$_4$-ReO$_3$ Structural Type Phase. In addition, their structures and electrochemical properties were investigated by X-ray diffraction (XRD) and galvanostatic charge-discharge test measurements (Saritha, 2018). Spontaneous Polarization of Fe-Doped SbNbO$_4$ Crystal was obtained experimentally (Shaldin, 2002).

2. Material and Methods

2.1. Structural optimization

The unit cell of the NbSbO$_4$ crystal with the *Pnma2$_1$* space group consists of 24 atoms. The unit cell of the NbSbO4 crystal is given in Figure 1 (Momma & Izumi, 2011). In the literature, the lattice parameters of the NbSbO$_4$ crystal are given as a= 9.55 Bohr, b= 10.73 Bohr, and c= 22.66 Bohr (Jain et al., 2013). Using these given lattice parameters, first, structural optimization was made for the unit cell of the NbSbO$_4$ crystal by means of the ABINIT (Gonze et al., 2002) package program within the framework of density functional theory. Self-consistent, norm-conversing pseudopotentials of the Trouillier-Martins type (Troullier & Martins, 1991) pseudo potentially generated by the FHI (FHI98PP) code (Fuchs & Scheffler, 1999) were used. Also, both the generalized gradient approximation (GGA) and the local density approximation (LDA) were used to solve the Khon-Sham equations (Kohn & Sham, 1965). As a result of the optimization, the cut-off energy value for both

GGA and LDA approximations was determined as 35 Hartree, as seen in Figure 2. In addition, the Brillouin Zone (BZ) 10×10×10 Monkhorst–Pack mesh grid was used for both the GGA and LDA approximations (Monkhorst & Pack, 1976). In addition, the volume value corresponding to the minimum energy value as a result of the optimization was calculated as 2415.8914 bohr^3 and 2208.3178 bohr^3 for both the GGA and LDA approximations, respectively. The energy-volume graph for the NbSbO₄ crystal is given in Figure 3.
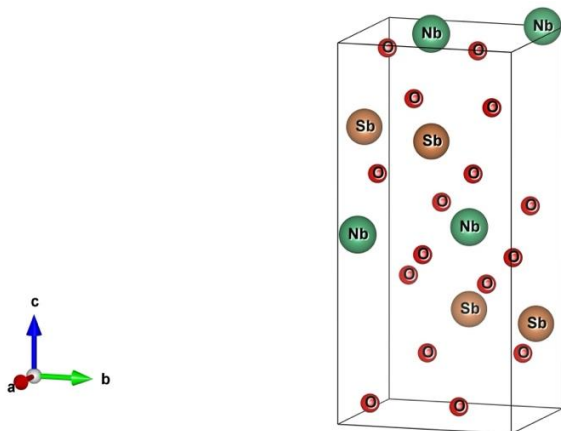

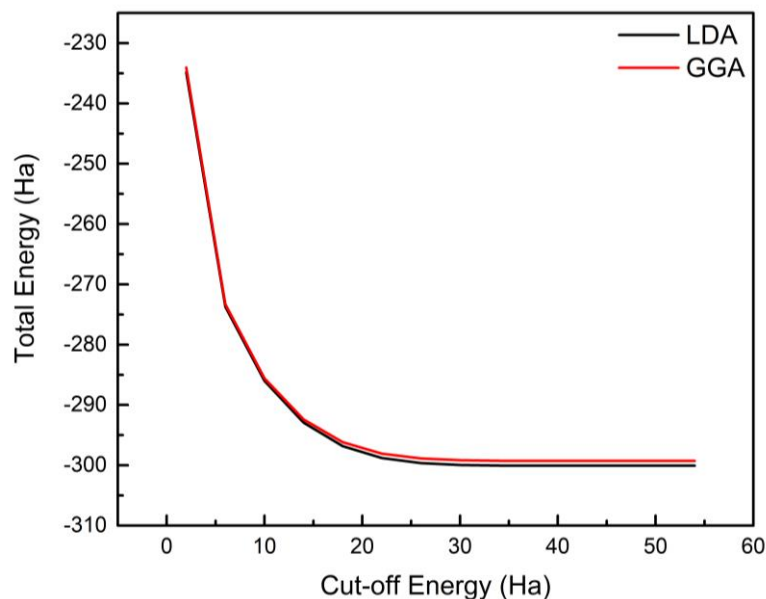Figure 1. The unit cell of NbSbO₄ crystal.

Figure 2. Cut-off energy curves for NbSbO₄ crystal under both GGA and LDA approximations.
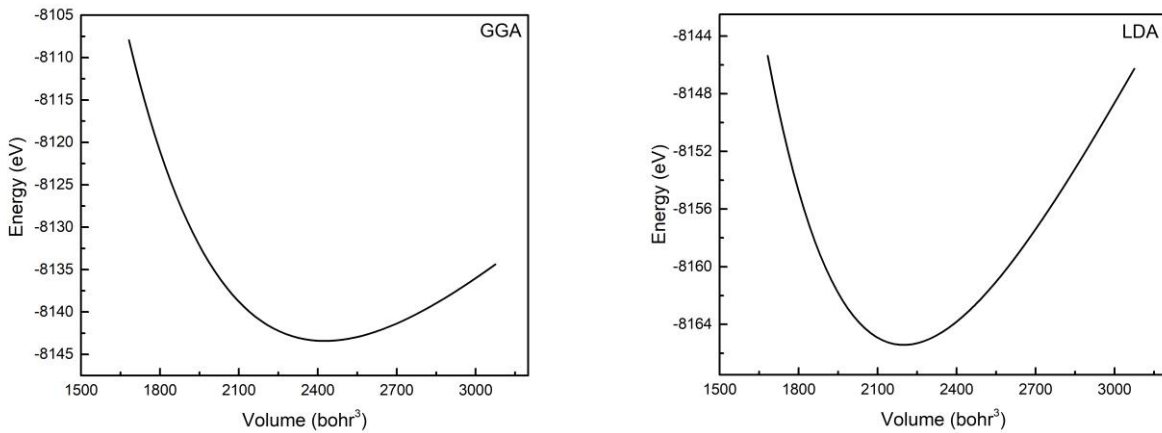
Figure 3. The curve of total energy volume of the primitive cell of NbSbO$_4$ crystal.

2.2. Elastic and piezoelectric properties

Then, the elastic stiffness tensor (C_{ij}) of the NbSbO$_4$ crystal in the ground state was calculated using the optimized lattice parameters. The independent components of the elastic constants vary according to the crystal structures (Nye, 1985). These components show the quantities associated with the material, such as stiffness, expansion, and shear deformations. The NbSbO$_4$ in orthorhombic crystal structure exhibits 9 independent components: C_{11}, C_{12}, C_{13}, C_{22}, C_{23}, C_{33}, C_{44}, C_{55}, and C_{66}. These calculated elastic constants (C_{ij}) for NbSbO$_4$ crystal are given in Table 1 and Table 2. The elastic compliance tensor (S_{ij}) of the NbSbO$_4$ crystal was calculated by means of these components. Then, using the components of C_{ij} and S_{ij} tensors, Bulk Modulus, Shear Modulus, Young Modulus, Poisson Ratio, Flexibility Coefficient, Debye temperature, Longitudinal sound wave velocity, Transverse sound wave velocity, and average speed of sound were calculated for the NbSbO$_4$ crystal. These calculated values for both GGA and LDA approximations are given in Table 3. For an ideal elastic incompressible material, the value of Poisson's ratio is 0.5. The Poisson ratio for most engineering materials ranges from 0.25 to 0.33. The Poisson ratio value is equal to 0.1 for covalent materials, 0.25 for ionic materials, and 0.33 for metallic materials (Köster & Franz, 1961).

The Poisson ratio calculated for the NbSbO$_4$ crystal under both the GGA and LDA approximations, respectively, is 0.276 and 0.278. Therefore, the NbSbO$_4$ crystal dominates an ionic crystal structure. Materials have a large stress value that will remain under the influence without deformation. This value is called the flexibility limit. When the flexibility limit is exceeded, the shape of the material changes, bends, or breaks. If the Flexibility Coefficient is greater than 1.75, the materials are ductile, otherwise, the material is one the brittle materials (Pugh, 1954). The Flexibility Coefficient calculated for NbSbO$_4$ crystal under both GGA and LDA approaches, respectively, is 1.90 and 1.92. This indicates that the NbSbO$_4$ crystal is a formable material.

Table 1. Elastic constants of NbSbO$_4$ crystal under GGA approximation (GPa)

C_{ij}	1	2	3	4	5	6
1	243.1	149.8	119.5	0	0	0
2	149.8	283	101.5	0	0	0
3	119.5	101.5	280.8	0	0	0
4	0	0	0	77.7	0	0
5	0	0	0	0	105.4	0
6	0	0	0	0	0	149.7

Table 2. Elastic constants of NbSbO$_4$ crystal under LDA approximation (GPa)

C$_{ij}$	1	2	3	4	5	6
1	311.4	197.2	162.9	0	0	0
2	197.2	356.1	130.3	0	0	0
3	162.9	130.3	386.6	0	0	0
4	0	0	0	100	0	0
5	0	0	0	0	143.5	0
6	0	0	0	0	0	199.4

Table 3. The elastic properties of NbSbO$_4$ crystal

Property	Symbol (Unit)	Value (GGA)	Value (LDA)
Voight Bulk Modulus	B$_V$ (GPa)	172	226
Reuss Bulk Modulus	B$_R$ (GPa)	172	226
Bulk Modulus VRH Average	B$_{VRH}$ (GPa)	172	226
Voight Shear Modulus	G$_V$ (GPa)	96	126
Reuss Shear Modulus	G$_R$ (GPa)	85	109
Shear Modulus VRH Average	G$_{VRH}$ (GPa)	90	118
Young Modulus	E (GPa)	231	301
Poisson Ratio	v (-)	0.276	0.278
Flexibility Coefficient	K (-)	1.90	1.92
Debye Temperature (K)	Θ_D	302.8	345.6
Longitudinal Sound Wave Velocity (v_l)	(m/s)	7005.9	8021.0
Transverse Sound Wave Velocity (v_t)	(m/s)	3896.1	4447.1
Average Speed of Sound (v_m)	(m/s)	4339	4954

Then, the piezoelectric properties of the NbSbO$_4$ crystal were investigated. To examine the piezoelectric properties of the NbSbO$_4$ crystal, geometric optimization was performed for the unit cell of the NbSbO$_4$ crystal, using the lattice parameters and atomic positions given in the literature. While making this calculation, the positions of the Nb atoms forming the unit cell of the NbSbO$_4$ crystal were kept constant. The positions of the remaining atoms and the lattice parameters were recalculated using the ABINIT package program. Parameters obtained under both GGA and LDA approximations are given in Table 4. The crystal's piezoelectric tensor (d_{ijk}) was calculated using the new lattice parameters and atomic positions calculated for the NbSbO$_4$ crystal. The number of independent components of the piezoelectric tensor varies depending on the number of axes of rotation and reflection of the crystal structures. The orthorhombic NbSbO$_4$ crystal belongs to the *mm2* point group. Hence the piezoelectric tensor for the NbSbO$_4$ crystal has five independent components. The calculated piezoelectric tensor of NbSbO$_4$ under different approximations is given in Table 5 and Table 6.

Table 4. Calculated lattice parameters and atomic positions for NbSbO$_4$ crystal

GGA a= 9.69 *Bohr*, b= 10.73 *Bohr*, c= 22.80 *Bohr*			LDA a= 9.29 *Bohr*, b= 10.30 *Bohr*, c= 21.89 *Bohr*		
x	*y*	*z*	*x*	*y*	*z*
0.5090	0.6125	0.4994	0.5090	0.6125	0.4994
0.4910	0.3875	0.9994	0.4910	0.3875	0.9994
0.9910	0.1125	0.4994	0.9910	0.1125	0.4994
0.0090	0.8875	0.9994	0.0090	0.8875	0.9994
0.4421	0.9751	0.2514	0.4494	0.9742	0.2516
0.5579	0.0249	0.7514	0.5506	0.0258	0.7516

Table 4. Calculated lattice parameters and atomic positions for NbSbO$_4$ crystal (continued)

GGA a= 9.69 *Bohr*, b= 10.73 *Bohr*, c= 22.80 *Bohr*			LDA a= 9.29 *Bohr*, b= 10.30 *Bohr*, c= 21.89 *Bohr*		
x	*y*	*z*	*x*	*y*	*z*
0.0579	0.4751	0.2514	0.0506	0.4742	0.2516
0.9421	0.5249	0.7514	0.9494	0.5258	0.7516
0.2277	0.8650	0.5476	0.2263	0.8556	0.5498
0.7723	0.1350	0.0476	0.7737	0.1444	0.0498
0.2723	0.3650	0.5476	0.2737	0.3556	0.5498
0.7277	0.6350	0.0476	0.7263	0.6444	0.0498
0.3333	0.6560	0.3391	0.3337	0.6493	0.3393
0.6667	0.3440	0.8391	0.6663	0.3507	0.8393
0.1667	0.1560	0.3391	0.1663	0.1493	0.3393
0.8333	0.8440	0.8391	0.8337	0.8507	0.8393
0.1695	0.8177	0.1519	0.1713	0.8217	0.1523
0.8305	0.1823	0.6519	0.8287	0.1783	0.6523
0.3305	0.3177	0.1519	0.3287	0.3217	0.1523
0.6695	0.6823	0.6519	0.6713	0.6783	0.6523
0.2077	0.5845	0.9379	0.2056	0.5920	0.9356
0.7923	0.4155	0.4379	0.7944	0.4080	0.4356
0.2923	0.0845	0.9379	0.2944	0.0920	0.9356
0.7077	0.9155	0.4379	0.7056	0.9080	0.4356

Table 5. Calculated piezoelectric constant for NbSbO$_4$ crystal under GGA approximation (C/m^2)

d_{ij}	1	2	3	4	5	6
1	0	0	0	0	-0.0135	0
2	0	0	0	-0.0062	0	0
3	0.0922	0.0918	-0.2110	0	0	0

Table 6. Calculated piezoelectric constant for NbSbO$_4$ crystal under LDA approximation (C/m^2)

d_{ij}	1	2	3	4	5	6
1	0	0	0	0	-0.0256	0
2	0	0	0	-0.0012	0	0
3	0.10032	0.1382	-0.2570	0	0	0

The piezoelectric effect is reversible, so removing the stress will eliminate the induced electric field. MTEX code (Bachmann et al., 2010) is a toolbox of comprehensive, freely available MATLAB software (The MathWorks Inc., 2020) that covers a wide variety of problems in texture analysis. The piezoelectric tensor (d) is a 3-rank tensor. Hence the piezoelectric tensor obeys the tensor transformation law of $_n$, which all third-order tensors obey. Where quantities such as a_{il} are the rotation matrices between d'_{ijk}, and d_{lmn}. This means that the crystal structure will remain unchanged when a rotation is applied over the point group to which it belongs (Nye, 1985). Here, piezoelectric representation surfaces for crystals can be studied by defining MTEX, Euler angles, quaternions, and axis/angle pairs. Piezoelectric properties for the crystal structure were

investigated with the help of MTEX using the calculated axis lengths, interaxial angles, and piezoelectric tensor for the NbSbO$_4$ crystal. x//a, y//b, and z//c for the cartesian coordinates given in the figures. Tensors can be represented geometrically. For example, 0th order tensors are sphere, 1st order tensors are vector, 2nd order tensors are quadric, 3rd order tensors are cubic, and 4th order tensors are quartic. In general, the representation surfaces of these tensors are given in Figure 4 (Newnham, 2005).
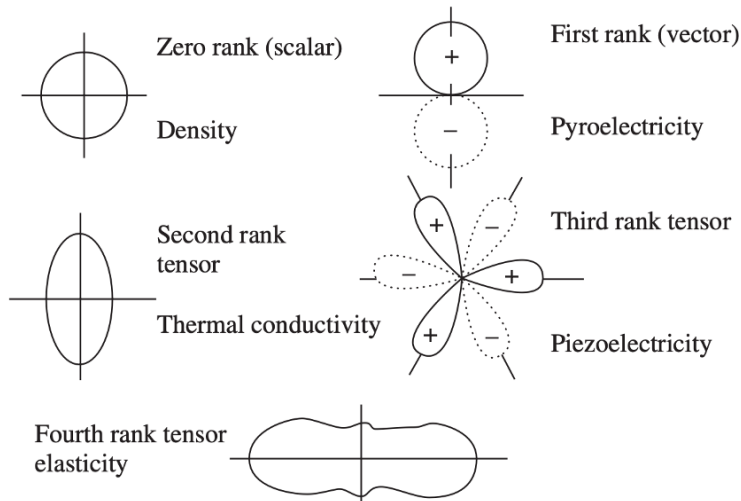

Figure 4. Representation surfaces for tensors.

The piezoelectric tensor can be visualized in various ways via MTEX. These visualizations are determined by the value of the piezoelectric tensor in the direction of the cartesian axes. With the '*section*' option of the MTEX drawing command, a longitudinal representation surface for a crystal with piezoelectric property in 2 dimensions can be drawn. The longitudinal piezoelectric representation surface of the NbSbO$_4$ crystal in 2 dimensions in different axes and under different approximations is calculated and given in Figure 5 and Figure 6. As seen in Figure 5 and Figure 6, there is no polarization in the regions outside the longitudinal limiting surfaces. In MTEX the magnitude of a piezoelectric tensor can be plotted as a function of crystal direction in the tensor frame on an equal area stereogram, either as the crystallographic asymmetric unit, as a complete hemisphere or even as both hemispheres. The plot of both hemispheres shows the 3D distribution of the piezoelectric tensor d values in *C/m²* (Mainprice et al., 2015). As can be seen in Figure 7 and Figure 8, the distributions of the upper and lower hemispheres are different under both the GGA and LDA approximations. The 3-D representation surface drawn with the piezoelectric tensor determines the maximum piezoelectric modulus of the material and the crystallographic direction in which this modulus arises. In cubic structures, this direction is clear. But that of other piezoelectric crystal classes is more complex. The 3-D piezoelectric tensor drawn for NbSbO$_4$ crystal under both GGA and LDA approximations is given in the C/m² unit in Figure 9 and Figure 10. The piezoelectric representation surfaces drawn for the NbSbO$_4$ crystal generally agree with the representation surfaces drawn for the *mm2* point group (De Jong et al., 2015).
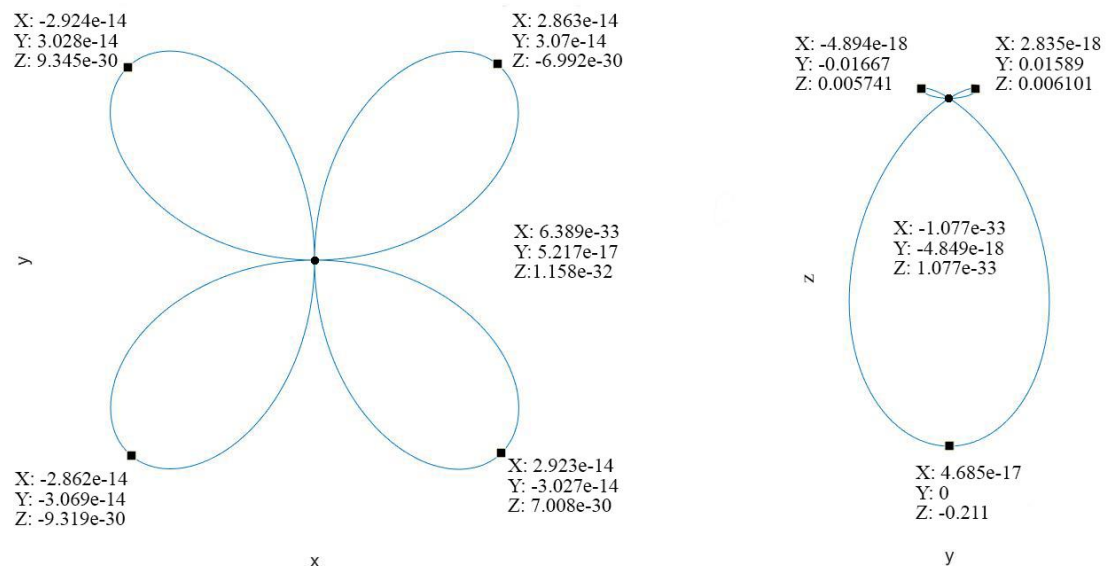
Figure 5. The plot of the longitudinal surfaces of the piezoelectric tensor for the NbSbO$_4$ crystal under the GGA approximation. Left side: z plane, Right side: x plane (Units: C/m^2).
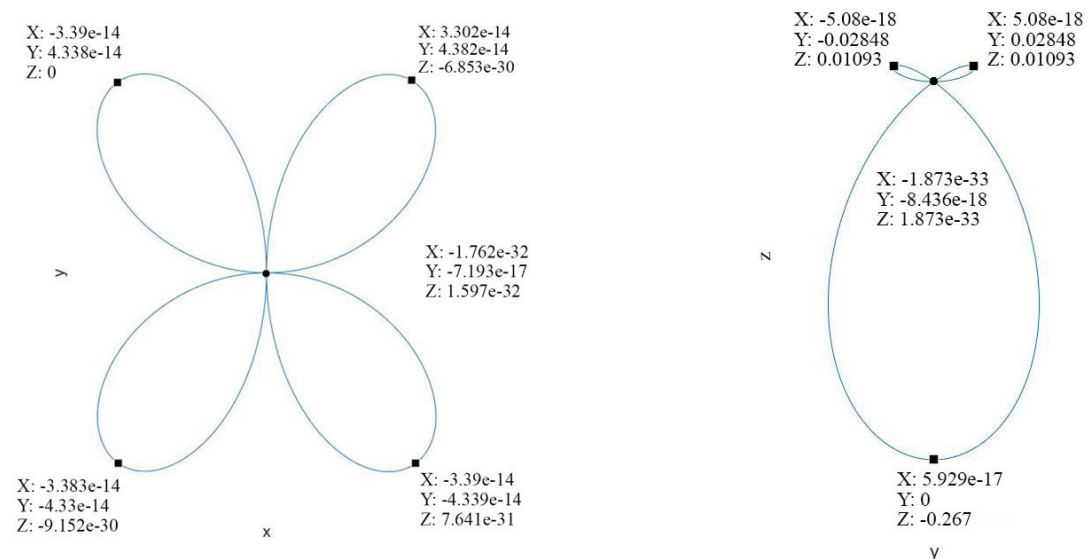

Figure 6. The plot of the longitudinal surfaces of the piezoelectric tensor for the NbSbO$_4$ crystal under the LDA approximation. Left side: z plane, Right side: x plane (Units: C/m^2).
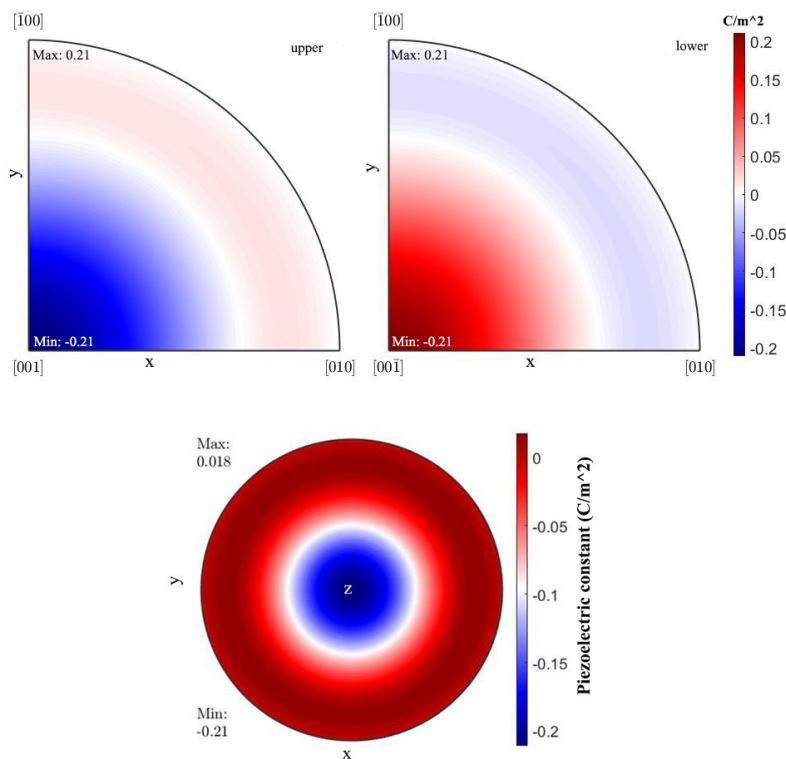
Figure 7. Plots of the piezoelectric tensor of the NbSbO$_4$ crystal under the GGA approximation of the upper, lower hemisphere, and full sphere in the x-y plane (Units: C/m^2).
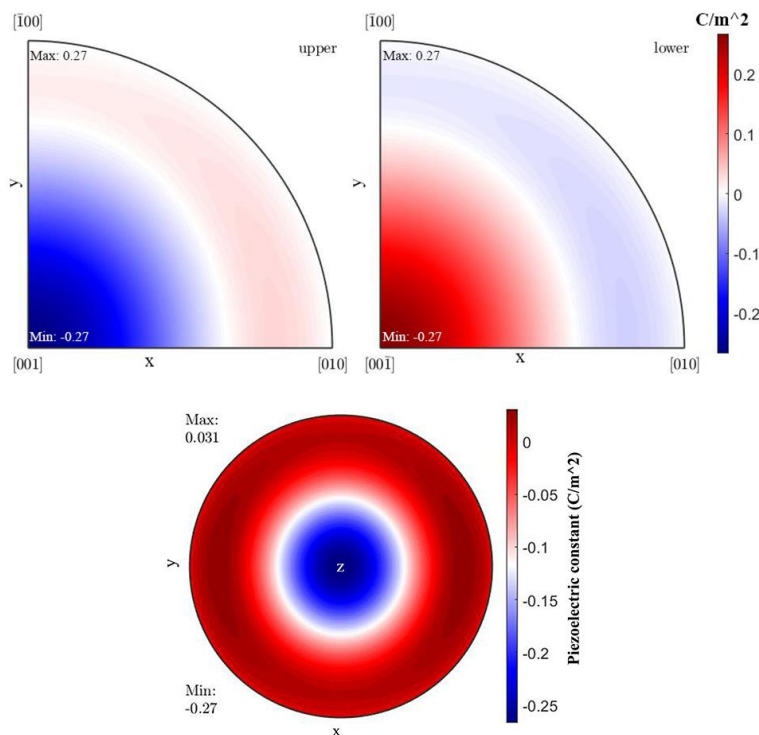
Figure 8. Plots of the piezoelectric tensor of the NbSbO$_4$ crystal under the LDA approximation of the upper, lower hemisphere, and full sphere in the x-y plane (Units: C/m^2).
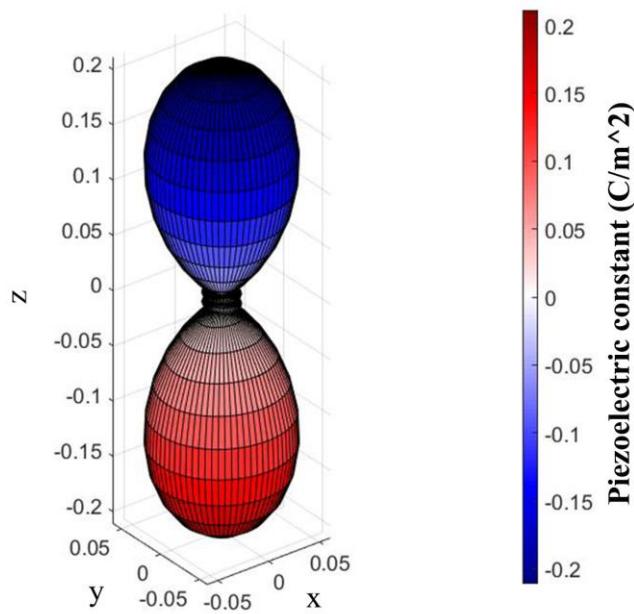
Figure 9. 3D drawing of the piezoelectric tensor for the NbSbO₄ crystal under the GGA approximation. It corresponds to the red (positive) and blue (negative) lobes (Units: C/m²).
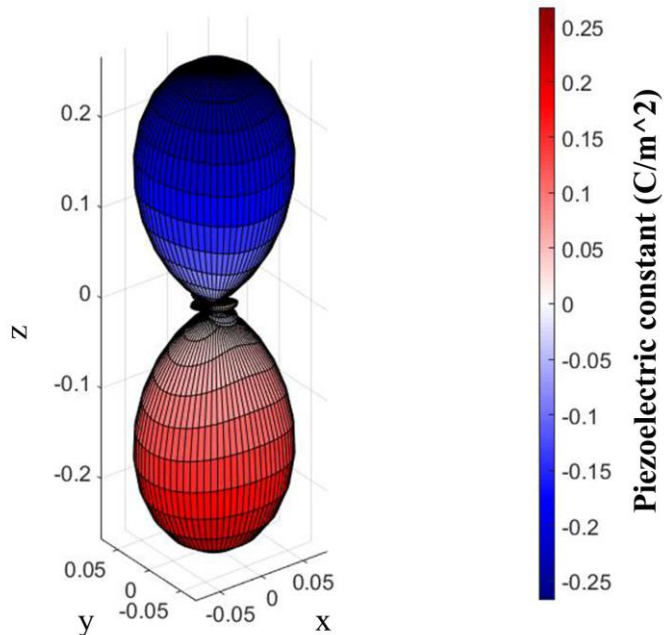

Figure 10. 3D drawing of the piezoelectric tensor for the NbSbO₄ crystal under the LDA approximation. It corresponds to the red (positive) and blue (negative) lobes (Units: C/m²).

3. Discussion and Conclusion

The structural, elastic, and piezoelectric properties of the orthorhombic NbSbO₄ crystal were calculated by density functional theory. Both GGA and LDA approximations and the ABINIT package program based on density functional theory were used for all calculations. First, structural optimization was performed for the NbSbO₄ crystal under GGA and LDA approximations, and the volume value corresponding to the minimum energy was obtained. Accordingly, the elastic properties of the NbSbO₄ crystal were calculated with the obtained lattice parameters. First, the elastic stiffness tensor and elastic compliance tensor were calculated under different approximations of the crystal.

Voigt Bulk Modulus (B$_V$), Reuss Bulk Modulus (B$_R$), Hill Bulk Modulus (B$_{VRH}$), Voigt Shear Modulus (G$_V$), Reuss Shear Modulus (G$_R$), Hill Shear Modulus (G$_{VRH}$), Young's Modulus for NbSbO$_4$ crystal (E), Poisson Ratio (ϑ), Coefficient of Elasticity (K), Debye temperature (Θ$_D$), Longitudinal sound wave velocity (υ$_l$), Transverse sound wave velocity (υ$_t$) and Average sound velocity (υ$_m$) were calculated. The data obtained for both approximations were compared. When the elastic properties of the material are examined, the elastic constants calculated with the LDA approximation are generally higher than the GGA approximation. The Debye temperature, known as the temperature at which the highest frequency mode is excited, was obtained under the LDA approximation with a temperature of 345.6 K, which was higher than the GGA approximation. Considering the Poisson ratios calculated under both the GGA and LDA approximations for the NbSbO$_4$ crystal, it was seen that the crystal was prone to ionic crystal structure under both approximations. Similarly, when the Flexibility Coefficients calculated for the NbSbO$_4$ crystal were compared under both approximations, it was seen that the NbSbO$_4$ crystal had a flexible and malleable structure. Finally, the piezoelectric tensor of the NbSbO$_4$ crystal was calculated. Accordingly, 2D longitudinal surfaces and 3D representation surfaces of the piezoelectric tensor were obtained using MTEX software. The distributions of the upper and lower hemispheres obtained with the piezoelectric tensor calculated under different approximations for the NbSbO$_4$ crystal were calculated differently under both GGA and LDA approximations. also, when looking at the values, the maximum values of the LDA approximation have higher values than those calculated for the GGA approximation. Similarly, when looking at the minimum values, it was seen that the values calculated for GGA were higher.

The calculations for both the GGA and LDA approximations for the NbSbO$_4$ crystal were compared. The differences of these two approximations on the material were revealed. I hope it will help future studies for NbSbO$_4$ crystal.

References

Ayyub, P., Multani, M. S., Palkar, V. R., & Vijayaraghavan, R. (1986). Vibrational spectroscopic study of ferroelectric SbNbO$_4$, antiferroelectric BiNbO$_4$, and their solid solutions. *Physical Review B*, 34(11), 8137. doi:10.1103/PhysRevB.34.8137

Bachmann, F., Hielscher, R., & Schaeben, H. (2010). Texture analysis with MTEX–free and open-source software toolbox. *Solid State Phenomena,* 160, 63-68. doi:10.4028/www.scientific.net/SSP.160.63

Bouty, E. (1883). Ueber die aktino-und piezo-elektrischen Eigenschaften des Bergkrystalles und ihre Beziehung zu den thermo-elektrischen (Sur les propriétés actino et piézo-électriques du quartz et leur relation avec ses propriétés pyro-électriques); Abh. der Sächs. Gesellschaft der Wissenschaften, t. XX, p. 459; 1881. *Journal of Physics: Theories and Applications*, 2(1), 89-93. doi:10.1051/jphystap:01883002008901

Chattopadhyay, S., Ayyub, P., Multani, M., & Pinto, R. (1998). Synthesis of oriented thin films of ferroelectric SbNbO$_4$ on Si by pulsed laser ablation. *Journal of Applied Physics*, 83(7), 3911-3913. doi:10.1063/1.366625

Curie, J., & Curie, P. (1880). Développement par compression de l'électricité polaire dans les cristaux hémièdres à faces inclinées. *Bulletin de Minéralogie*, 3(4), 90-93. doi:10.3406/bulmi.1880

De Jong, M., Chen, W., Geerlings, H., Asta, M., & Persson, K. A. (2015). A database to enable discovery and design of piezoelectric materials. Scientific *Data*, 2(1), 1-13. doi:10.1038/sdata.2015.53

Dineva, P., Gross, D., Müller, R., & Rangelov, T. (2014). Piezoelectric materials. In *Dynamic Fracture of Piezoelectric Materials (*pp. 7-32). Springer, Cham. doi:10.1007/978-3-319-03961-9_2

Dulian, P., Piz, M., Filipek, E., & Wieczorek-Ciurowa, K. (2014). Comparative study of phases forming in niobium-antimony oxides system upon high temperature treatment and high-energy ball milling. *Acta Physica Polonica A*, 126(4), 938-942. doi:10.12693/APhysPolA.126.938

El-Fadl, A. A., Mohamad, G. A., & Yamazaki, T. (2003). Variation of the absorption spectra and optical energy gap with γ-ray irradiation and heat treatment in SbNbO$_4$ films deposited on MgO and quartz substrates. *Materials Chemistry and Physics*, 80(1), 239-249. doi:10.1016/S0254-0584(02)00464-9

Fuchs, M., & Scheffler, M. (1999). Ab initio pseudopotentials for electronic structure calculations of poly-atomic systems using density-functional theory. *Computer Physics Communications*, 119(1), 67-98. doi:10.1016/S0010-4655(98)00201-X

Fukunaga, O., & Yamaoka, S. (1979). Phase transformations in ABO$_4$ type compounds under high pressure. *Physics and Chemistry of Minerals*, 5(2), 167-177. doi:10.1007/BF00307551

Gonze, X., Beuken, J. M., Caracas, R., Detraux, F., Fuchs, M., Rignanese, G. M., … & Allan, D. C. (2002). First-principles computation of material properties: the ABINIT software project. *Computational Materials Science*, 25(3), 478-492. doi:10.1016/S0927-0256(02)00325-7

Jain, A., Ong, S. P., Hautier, G., Chen, W., Richards, W. D., Dacek, S., … & Persson, K. A. (2013). Commentary: The Materials Project: A materials genome approach to accelerating materials innovation. *APL Materials*, 1(1), 011002. doi:10.1063/1.4812323

Kim, S. H., Park, S., Lee, C. W., Han, B. S., Seo, S. W., Kim, J. S., Cho, I. S., & Hong, K. S. (2012). Photophysical and photocatalytic water splitting performance of stibiotantalite type-structure compounds, SbMO$_4$ (M= Nb, Ta). *International Journal of Hydrogen Energy*, 37(22), 16895-16902. doi:10.1016/j.ijhydene.2012.08.123

Knauth, P., & Schwitzgebel, G. (1988). Calorimetric investigations on the SbNbO$_4$-SbSbO$_4$ system. *Journal of Thermal Analysis*, 33(3), 619-623. doi:10.1007/BF02138564

Knauth, P., & Schwitzgebel, G. (1990). Thermodynamic properties of antimony (III) niobate (V). *The Journal of Chemical Thermodynamics*, 22(5), 481-485. doi:10.1016/0021-9614(90)90140-L

Kohn, W., & Sham, L. J. (1965). Self-consistent equations including exchange and correlation effects. *Physical Review*, 140(4A), A1133. doi:10.1103/PhysRev.140.A1133

Köster, W., & Franz, H. (1961). Poisson's ratio for metals and alloys. *Metallurgical Reviews*, 6(1), 1-56. doi:10.1179/mtlr.1961.6.1.1

Mainprice, D., Bachmann, F., Hielscher, R., Schaeben, H., & Lloyd, G. E. (2015). Calculating anisotropic piezoelectric properties from texture data using the MTEX open-source package. *Geological Society, London, Special Publications*, 409(1), 223-249. https://doi.org/10.1144/SP409.2

Mohamed, G. A., Yamazaki, T., Nakatani, N., Yuhara, J., & Morita, K. (1998). Growth and optical properties of SbNbO$_4$ films. *Ferroelectrics*, 218(1), 199-208. doi:10.1080/00150199808227147

Mohamad, G. A., El-Fadl, A. A., & Yamazaki, T. (2001). Effect of gamma irradiation and heat treatment on the optical properties of SbNbO$_4$ ferroelectric thin films. *Radiation Effects and Defects in Solids*, 154(2), 165-178. doi:10.1080/10420150108214050

The MathWorks Inc. (2020). MATLAB version: 9.9.0.1 (R2020b), Natick, Massachusetts: The MathWorks Inc. https://www.mathworks.com

Momma, K., & Izumi, F. (2011). VESTA 3 for three-dimensional visualization of crystal, volumetric and morphology data. *Journal of Applied Crystallography*, 44(6), 1272-1276. doi:10.1107/S0021889811038970

Monkhorst, H. J., & Pack, J. D. (1976). Special points for Brillouin-zone integrations. *Physical Review B*, 13(12), 5188. doi:10.1103/PhysRevB.13.5188

Müller, O., & Roy, R. (1973). Phase transitions among the ABX$_4$ compounds. *Zeitschrift für Kristallographie-Crystalline Materials*, 138(1-6), 237-253. doi:10.1524/zkri.1973.138.jg.237

Newnham, R. E. (2005). *Properties of Materials: Anisotropy, Symmetry, Structure*. Oxford University Press.

Nye, J. F. (1985). *Physical Properties of Crystals: Their Representation by Tensors and Matrices*. Oxford University Press.

Popolitov, V. I., Ivanova, L. A., Stephanovitch, S. Y., Chetchkin, V. V., Lobachev, A. N., & Venevtsev, Y. N. (1974). Ferroelectrics abo4: Synthesis of single crystals and ceramics; dielectric and nonlinear optical properties. *Ferroelectrics*, 8(1), 519-520. doi:10.1080/00150197408234145

Popolitov, V. I., Lobachev, A. N., & Peskin, V. F. (1982). Antiferroelectrics, ferroelectrics and pyroelectrics of a stibiotantalite structure. *Ferroelectrics*, 40(1), 9-16. doi:10.1080/00150198208210591

Pugh, S. F. (1954). XCII. Relations between the elastic moduli and the plastic properties of polycrystalline pure metals. *The London, Edinburgh, and Dublin Philosophical Magazine and Journal of Science*, 45(367), 823-843. doi:10.1080/14786440808520496

Qu, X. X., & Lévy, F. (1995). Textured ferroelectric $SbNbO_4$ thin films deposited by ion-beam sputtering. *Ferroelectrics Letters Section*, 20(3-4), 83-88. doi:10.1080/07315179508204287

Rannev, N. V., Shchedrin, B. M., & Venevtsev, Y. N. (1976). Crystal structure of ferrielectric stibiumniobite SbNbO4. *Ferroelectrics*, 13(1), 523-525. doi:10.1080/00150197608236657

Saritha, D. (2018). Electrochemical reaction of lithium with $SbNbO_4$-ReO_3 structure type phase. *Materials Today: Proceedings*, 5(9), 17579-17584. doi:10.1016/j.matpr.2018.06.075

Shaldin, Y. V. (2002). Spontaneous polarization of Fe-doped $SbNbO_4$ crystals. *Crystallography Reports*, 47(3), 484-488. doi:10.1134/1.1481939

Troullier, N., & Martins, J. L. (1991). Efficient pseudopotentials for plane-wave calculations. *Physical Review B*, 43(3), 1993. doi:10.1103/PhysRevB.43.1993